Novel catalytic behavior of Cu/Al_2O_3 catalyst against daily start-up and shut-down (DSS)-like operation in the water gas shift reaction

Shun Nishimura,[b] Tetsuya Shishido,*[a] Kohki Ebitani,[b] Kentaro Teramura,[c]

and Tsunehiro Tanaka[a]

Affiliations

[a] *Department of Molecular Engineering, Graduate School of Engineering, Kyoto University, Katsura, Kyoto 615-8510, Japan.*
[b] *School of Materials Science, Japan Advanced Institute of Science and Technology, Nomi, Ishikawa 923-1292, Japan.*
[c] *Kyoto University Pioneering Research Unit for Next Generation, Kyoto University, Katsura, Kyoto 615-8510, Japan.*

Corresponding author

Dr. Tetsuya Shishido
Department of Molecular Engineering, Graduate School of Engineering, Kyoto University, Katsura, Kyoto 615-8510, Japan.
Tel: +81 75 383 2559
Fax: +81 75 383 2561
E-mail: shishido@moleng.kyoto-u.ac.jp

Abstract

Cu/Al_2O_3 catalysts (Cu/Al=1/2) have been prepared by co-precipitation (CP-), homogeneous precipitation (HP-), sol-gel (SG-), and impregnation (IMP-) methods. Prepared Cu/Al_2O_3 catalysts were applied to the water gas shift (WGS) reaction. Effects of preparation method and calcination temperature on their activities for the WGS reaction and sustainability against the daily start-up and shut-down (DSS)-like operation between 323-473 K under steam treatment were investigated. CP-, HP-, and SG-Cu/Al_2O_3 catalysts showed a sustainable activity during DSS-like operation in the WGS reaction, whereas IMP-Cu/Al_2O_3 showed a quite low sustainability. CP-Cu/Al_2O_3 catalyst calcined at 823 K (CP-823) showed the highest activity and sustainability among the catalysts tested and almost similar to a commercial $Cu/ZnO/Al_2O_3$ catalyst (MDC-7) even after 50 cycles of the DSS-like operation in the WGS reaction. In contrast, CP-Cu/Al_2O_3 catalyst calcined at 1073 K (CP-1073) showed a low sustainability, although the initial activity was higher than that of CP-823. It was concluded that such prominent performances of the CP-823 catalyst is caused by 1) the formation of highly dispersed and stable Cu metal and 2) an important role of boehmite (AlO(OH)) phase formed during the DSS operation in inhibition of aggregation of Cu metal particles. For CP-1073 K, "*in-situ*" formation of boehmite phase did not proceed due to the formation of stable $CuAl_2O_4$ phase by calcination at high temperature. Therefore, the activity of CP-1073 remarkably decreased as a result of aggregation of Cu metal particles during the DSS-like operation.

Key Words: Water gas shift reaction, DSS operation, Cu/Al_2O_3 catalyst, High sustainability, Boehmite.

1. Introduction

The cogeneration system with the polymer electrolyte membrane fuel cells (PEMFCs) using H_2 fuel is attractive as a new energy system because of their high power density, low temperature operation, low emissions of NOx, greenhouse gas and so on [1, 2]. Many researchers have studied the method of the production of hydrogen by the reforming of hydrocarbons like methane, propane, methanol, and kerosene [3-6]. When hydrogen is supplied to PEMFCs by reforming hydrocarbons, it is necessary to remove CO because it poisons the Pt electrode of PEMFCs and decreases their activity for electrochemical reaction. The water-gas shift (WGS) reaction is promising for removing CO from reformer gas [7, 8], since it is moderately exothermic reaction (ΔH_{298} = -41.1 kJ mol^{-1}) and the reaction temperature is easy to control. The equilibrium conversion of CO is dependent largely on the reaction temperature. Since the WGS reaction is moderately exothermic reaction, lower temperature is favored for higher CO removal. On the other

hand, from the viewpoint of kinetics, the reactant gases are not active enough to reach the chemical equilibrium at low temperature.

Since daily start-up and shut-down (DSS) operations are envisaged for residential applications of PEMFCs systems, the catalysts for the WGS reaction are sometimes exposed to water and/or oxygen containing atmosphere at low temperatures, and the catalytic activity decreases as a result of oxidation and/or aggregation of active species [9, 10]. For this reason, high sustainability against fluctuation from oxidative to reductive atmospheres in addition to high activity is essential for the catalysts for the WGS reaction. Generally, the activity of copper-based catalysts is higher for this reaction [11-18], but is less stable to oxidant gases than precious metal like Pt, Ru and Au. Therefore, it is important to develop highly stable Cu-based catalysts or highly active precious metal catalysts. Recently, various ceria supported metal catalysts have been prepared and used in the WGS reaction. Cu/CeO_2 and Ni/CeO_2 were prepared by the urea coprecipitation-gelation [19], Pd/CeO_2 was prepared by impregnation [20], Au/CeO_2 was prepared by deposition–precipitation [21], and both Au/CeO_2 [22] and $Cu\text{-}Pd/CeO_2$ catalysts [23] were prepared by the urea coprecipitation-gelation method. However, Zalc et al. [24] reported that a large amount of H_2 leads to the irreversible reduction of CeO_2

and the catalyst deactivation. Pt/TiO_2 [25] and Pt/Al_2O_3 [26] were promising candidate as the catalysts for low-temperature WGS reaction. Ru was also active for the WGS reaction. Ru/V_2O_3 catalyst was prepared by the reduction of Ru/V_2O_5 at 673 K in H_2 [27] and Ru/hydroxyapatite catalyst was prepared by deposition-precipitation method [28]. Ternary $Cu/ZnO/Al_2O_3$ catalysts have been widely employed commercially since the early 1960s in the WGS reaction; the catalyst was usually prepared by coprecipitation method to afford the higher Cu metal dispersion in the resulting catalyst and, as a consequence, the higher catalytic activity [11]. Coprecipitated $Cu/ZnO/Al_2O_3$ catalysts were more sustainable than the impregnated catalysts in the shift reaction [29]. The formation of spinel phase such as Cu-Al, Cu-Mn, and Cu-Fe systems [12-14], CeO_2 impregnation [15], and MgO doping [16] have been proposed to improve the stability of Cu-based catalyst. In addition, a variety of preparation methods such as coprecipitation and sol-gel methods have been also investigated [12, 13, 16]. However, further effort to improve the stability of Cu-based catalysts is still necessary. Moreover, it is important to elucidate the mechanisms of improvement of sustainability by the additives and deactivation.

Recently, we reported that an unique and novel behavior and high sustainability of simple binary Cu/Al_2O_3 catalysts, prepared from homogeneous precursors and calcined at

low temperature, against the DSS-like operation in the WGS reaction [18]. The Cu/Al_2O_3 catalyst prepared by coprecipitation shows high activity and sustainability even after 50 cycles of DSS-like operation. A mechanism of improvement of sustainability by "*in-situ*" formation of boehmite (AlO(OH)) phase is proposed. In this present study, the effects of preparation method and calcination temperature of simple Cu/Al_2O_3 catalyst on their activities for the WGS reaction and sustainability against the DSS-like operation were investigated. We demonstrate that the relationship between the catalytic performance (activity and durability) and the change in structure of Cu/Al_2O_3 catalysts during the reaction by using XRD, TEM, HRTEM, N_2O decomposition, and Cu K-edge XAFS techniques in order to demonstrate the important role of "*in-situ*" formed boehmite in improvement of sustainability against DSS operation.

2. Experimental

2.1 Catalyst preparation

Cu/Al_2O_3 catalysts (Cu/Al=1/2) were prepared by coprecipitation (CP-), homogeneous preparation (HP-), sol-gel (SG-) and impregnation (IMP-) methods. The Cu loading in these Cu/Al_2O_3 catalysts was 5.5 mmol g^{-1}.

Co-precipitation method (CP-) CP-catalysts were prepared by coprecipitation, i.e., the aqueous solution of metal nitrates was dropped into aqueous solution of Na_2CO_3 with vigorous stirring and the pH was adjusted at 9 with NaOH. The obtained precipitate was aged at 333 K for 24 h, filtered, washed with distilled water, and dried at 373 K for overnight.

Homogeneous precipitation method (HP-) HP-catalysts were prepared by using urea hydrolysis [30-32] as follows: urea was mixed into a solution of metal nitrates at room temperature, and the urea was hydrolyzed by heating the mixture at 363 K. During the hydrolysis of urea, hydroxide ions are generated in the homogeneous solution (Eq. (1)).

$$CO(NH_2)_2 + 3H_2O \rightarrow 2NH_4^+ + HCO_3^- + OH^- \quad (1)$$

The precipitates were then filtered, washed, and dried in air at 373K.

Sol-gel method (SG-) SG-catalysts were prepared by the citrate sol-gel method [33,34]. Two kinds of aqueous solutions of copper and aluminum nitrate were treated with an excess amount of citric acid and ethylene glycol and then each solution was mixed. This mixture was evaporated at 348 K to make a sol of the organometallic complex.

Impregnation method (IMP-) IMP-catalysts were prepared by an impregnation method using γ-Al_2O_3 (164 m^2 g^{-1}, JRC-ALO-8) and Cu nitrate solution. IMP-Cu/AlO(OH) was

also prepared by impregnation and calcined at 823 K in air for 3 h. AlO(OH) (265 m^2 g^{-1}, Wako) was used as the support and impregnated with Cu nitrate aqueous solution. The Cu loading on IMP-Cu/AlO(OH) is similar to those of Cu/Al_2O_3 catalysts.

The catalysts were obtained by calcining the precipitates at 573-1173 K in air (abbreviated as CP-*X*, where *X* is the calcination temperature).

2.2 Characterization

The structure of prepared catalyst was studied by using XRD, TEM, H_2-TPR, N_2 adsorption and N_2O decomposition methods.

XRD patterns of the catalysts were recorded using a Rigaku Rint 1000 instrument, with mono-chromatized Cu Kα radiation (λ = 0.154 nm) at 40 kV and 20 mA. The diffraction pattern was identified by comparing with those in the JCPDS (Joint Committee of Powder Diffraction Standards) database. The mean crystallite size was determined according to the Scherrer equation. The change in the morphology of the catalyst was observed by transmission electron microscope (TEM). TEM, high-resolution TEM and energy dispersive X-ray spectroscopy (EDS) measurements were performed with Hitachi H-7100 and JEOL JEM-2100F. The H_2-TPR profiles recorded using an Ohkura BP-2

instrument were used for determination of H_2 consumption for reduction of Cu species in Cu/Al_2O_3 catalysts. The fresh catalysts were oxidized with O_2 at 573 K for 1 h prior to determination of the TPR profile. After the reduction at 523 K and the DSS-like operation, the catalysts were cooled to room temperature in N_2. The catalysts were mounted in quartz tubes in air and heated in 5 vol. % H_2 diluted with argon without any pretreatment at a heating rate of 10 K min^{-1}. The gas was purified by passing through both 13X molecular sieves for removal of trace amount of water and MnO_2 for removal of trace amount of oxygen. The change in the H_2 concentration was monitored by a thermal conductivity detector (TCD). Since water is formed during the reduction process, the effluent gas from the reactor was dried over 5A molecular sieves before entering the TCD. The amount of consumed H_2 was quantified by a calibration curve method. BET surface areas of samples were determined by using N_2 adsorption isotherm at 77 K with COULTER SA3100. The copper metal surface areas were determined by N_2O decomposition method as reported by Evans et al. [35], assuming a reaction stoichiometry of two Cu atoms per oxygen atom and a Cu surface density of 1.68 $\times 10^{19}$ Cu atom m^{-2}. Prior to the measurement, sample was reduced at 523 K for 0.3 h in H_2/N_2 (5.0 vol. % H_2, flow rate; 20 ml min^{-1}) mixed gas flow.

2.3 Catalytic reactions and analyses of the products

The WGS reaction was carried out using a fixed bed reactor at atmospheric pressure with $CO/CO_2/H_2O/H_2$ (7.3/7.3/27.2/58.3) mixed gas at 473 K. Prior to the WGS reaction, 0.2 g of the catalysts were reduced with 5 vol.% H_2 diluted with nitrogen at 523 K for 0.5 h. The products were analyzed using two on-line gas chromatographs (GC). A GC with packed Molecular Sieve 5A column, Ar carrier gas and TCD were used to analyze H_2. Another GC with packed Porapak-Q column, N_2 carrier gas and FID with methanizer were used to analyze CO and CO_2. The conversion of CO was quantified by a calibration curve method and the following equation (Eq. (2)).

$$C\ O\ o\ n\ v = \left[\frac{C\ O_{in} - C\ O_{out}}{C\ O_{in}}\right] \times 100 \qquad (2)$$

As a DSS-like operation, steam treatment in H_2O/N_2 (25.1/74.9) was repeated over the temperature range of 323-473 K (Fig. 1). After this DSS-like operation, the WGS reaction was carried out again and CO conversion was compared with that of fresh catalyst. A commercial $Cu/ZnO/Al_2O_3$ catalyst, MDC-7 (Cu loading, estimated by XRF, was almost similar to those of prepared Cu-Al-Ox catalysts, 5.4 $mmolg^{-1}$.), was used as a reference.

2.4 *In-situ* time-resolved XAFS

In-situ time-resolved Cu *K*-edge X-ray absorption spectra (XAS) were measured on the beam line BL01B1 at SPring-8 of the Japan Synchrotron Radiation Research Institute (Proposal No. 2007B1123 and 2008A1147), Japan in a transmission mode at room temperature by using two ion chambers. The storage ring was operated at 8 GeV with injection currents of 100 mA. Si(111) single crystal is used to obtain a monochromatic X-ray beam. The wafer of the sample diluted with boron nitride (Wako) was mounted in an *in-situ* flow cell designed by Suzuki and Nomura [36]. Cu K-edge XAFS spectra were measured in the Quick-XAFS (QXAFS) mode with a time resolution of 60 s $spectrum^{-1}$ (8723-10362 eV). Scheme of *in-situ* experiment was shown in Fig. 2. First the catalysts were reduced with 5 vol.% H_2 diluted with helium from room temperature to 633 K with a ramping rate of 5 K min^{-1}. Then, the WGS reaction was carried out with $CO/CO_2/H_2O/H_2$ (7.3/7.3/27.2/58.3) mixed gas at 473 K for 0.5 h. Next, as a DSS-like operation, steam treatment in H_2O/He (25.1/74.9) was carried out over the temperature range of 323-473 K. After this DSS-like operation, the WGS reaction was carried out again. Data are analyzed by means of the REX2000 program (Version: 2.5.7; Rigaku Corp.). The oscillation is normalized by the edge height around 70-100 eV higher than the threshold. Identification of the number of phases was achieved by factor analysis of observed XANES spectra.

Factor analysis of a series of XANES spectra were performed with Specfit ver. 2.12 for MS-DOS. References spectra of Cu metal, Cu_2O and CuO were then used in a least-squares fitting procedure of the time-resolved spectra to determine the fraction of each phase present.

3. Results and discussion

3.1. Effect of calcination temperature on the initial activity

Fig. 3 shows the XRD patterns of CP- and IMP-Cu/Al_2O_3 before and after calcination at various temperatures. The diffraction lines of hydrotalcite-like compound (JCPDS 89-0460) were observed in the XRD patterns of the CP-Cu/Al_2O_3 after drying at 373 K (Fig. 3 A (a)). The intensity of the diffraction lines of CuO (JCPDS 48-1548) and $CuAl_2O_4$ spinel phase (JCPDS 73-1958) increased with increasing the calcination temperature. The XRD pattern of CP-1173 catalysts showed diffraction lines of well crystallized $CuAl_2O_4$ spinel phase and weak lines of CuO, suggesting that the most part of Cu^{2+} was dispersed uniformly in a spinel structure. In the case of IMP-Cu/Al_2O_3 catalysts, the calcination up to 973 K did not cause the formation of $CuAl_2O_4$ spinel phase crystallite. Above 1023 K, strong diffraction lines of CuO together with lines of spinel $CuAl_2O_4$

phase were found. The intensity of the diffraction lines of $CuAl_2O_4$ spinel phase increased with increasing the calcination temperature. The intensity and width of the lines of CuO on IMP-1173 was much stronger and narrower than those on CP-1173, indicating that the crystallite size of CuO on IMP-1173 was larger than that on CP-1173.

TPR profiles of CP- and IMP-Cu/Al_2O_3 catalysts calcined at various temperatures are shown in Fig. 4. The numbers by peaks are the amount of H_2 consumed (mmol g^{-1}). Although the reduction of bulk γ-Al_2O_3 is thermodynamically feasible at high temperatures, γ-Al_2O_3 showed no distinct peak of the reduction up to 800 K (data not shown). IMP-823 catalyst showed a single H_2 consumption peak at 560 K with a small shoulder around 580 K, which is assignable to reduction of Cu^{2+} in bulk CuO to Cu^0 with a large distribution of particle size [14, 37-39]. When the calcination temperature increased up to 1023 K, the H_2 consumption peak shifts to slightly lower temperature (ca. 510 and 530 K) and the amount of H_2 consumed slightly decreased. When the IMP-Cu/Al_2O_3 catalysts were calcined above 1023 K, a small H_2 consumption peaks appeared at 510 K and around 730 K. These two peaks are assignable to the reduction of highly dispersed CuO and $CuAl_2O_4$ spinel phase, respectively [14]. The amount of H_2 consumed around 560 K decreased with increasing the calcination temperature. These

results indicate that bulk CuO was transformed to highly dispersed CuO and $CuAl_2O_4$ spinel phase by calcination at high temperature. CP-823 and 873 catalysts show two H_2 consumption peaks. CP-973 showed a H_2 consumption peak at 525 K with small peak at 680 K, and the former peak shifted to slightly lower temperature by increasing the calcination temperature up to 973 K. Luo et al. reported that the reduction temperature of highly dispersed CuO species was lower than that of bulk CuO species using H_2-TPR combined with *in-situ* XRD [40]. It appears that the shift of H_2 consumption peak to lower temperature is due to the improvement of the dispersion of CuO species. The H_2 consumption peak temperature of CP-973 (525 K) was lower than that of IMP-973 (560 K), suggesting that the dispersion of CuO on CP-973 was higher than that on IMP-973. These results correspond with the copper metal surface area (Cu^0 surface area) (*vide infra*). CP-1073 and 1173 showed two H_2 consumption peaks around 490 K and broad peak around 690 K. The amount of H_2 consumption around 490 K of CP-1173 is smaller than that at 525 K of CP-973. This suggests that the amount of highly dispersed CuO species over CP-1173 is smaller than that of CP-973.

Fig. 5 shows the activities in the WGS reaction and Cu^0 surface area determined by N_2O pulse method of CP- and IMP-Cu/Al_2O_3 catalysts calcined at various temperatures. In

the case of CP-Cu/Al_2O_3 catalysts, CO conversion increased up to 973 K and then remarkably decreased. The change in Cu^0 surface area against the calcination temperature correlates with the change in CO conversion, suggesting Cu^0 as the active species. On the basis of TPR profiles, it is likely that the amount of CuO particles can be reduced at lower temperature affected to the catalytic activity. HP- and SG-catalysts showed almost similar change in the XRD pattern, CO conversion, and Cu^0 surface area (see Figs. S1 and S2). In the case of IMP-Cu/Al_2O_3 catalysts, IMP-973 showed the highest CO conversion among IMP-Cu/Al_2O_3 catalysts tested, whereas the magnitude of the changes in Cu^0 surface area was not very large. These results suggest that the formation of $CuAl_2O_4$ spinel phase by calcination at high temperatures (above 1023 K) affects the catalytic activity.

3.2.Effect of calcination temperature on the sustainability

Both CP- and IMP-Cu/Al_2O_3 catalysts were calcined at 823 and 1073 K and the effect of the DSS-like operation on the sustainability for the WGS reaction was tested. Time course of the WGS reaction before and after 10 cycles of DSS-like operation over CP- and IMP-Cu/Al_2O_3 catalysts together with a commercial $Cu/ZnO/Al_2O_3$ catalyst (MDC-7) are shown in Fig. 6. Before DSS-like operation, Cu/Al_2O_3 catalysts calcined at

1073 K showed higher CO conversion those calcined at 823 K. The commercial $Cu/ZnO/Al_2O_3$ catalyst showed higher activity than Cu/Al_2O_3 catalysts. The activities of CP-1073, IMP-823, IMP-1073, and the commercial $Cu/ZnO/Al_2O_3$ catalyst remarkably decreased after DSS-like operation. Surprisingly, the activity of CP-823 was remarkably improved by DSS-like operation, and moreover the activity of this catalyst was almost similar to that of the commercial ternary $Cu/ZnO/Al_2O_3$ catalyst.

Fig. 7 shows the activities and BET surface areas of Cu/Al_2O_3 catalysts calcined at 823 and 1073 K, together with a commercial $Cu/ZnO/Al_2O_3$ catalyst (MDC-7), in the WGS reaction before and after the DSS-like operation. The BET surface areas of Cu/Al_2O_3 catalysts calcined at 1073 K and MDC-7 were almost constant before and after the DSS-like operation in spite of the preparation method. In the case of HP-1073, CO conversion decreased slightly after the first DSS-like operation and decreased drastically after 10 cycles. CP-1073, SG-1073, and IMP-1073 showed similar behavior, indicating that the spinel $CuAl_2O_4$ phase cannot prevent deactivation during the DSS-like operation. IMP-823 showed significant deactivation immediately after the first DSS-like operation, suggesting that Cu metal was immediately oxidized and/or aggregated by steam. The activity of MDC-7 also decreased drastically with increase in the number of cycles of

DSS-like operation. By contrast, HP-823 and SG-823 exhibited improved CO conversion with increasing number of cycles of DSS-like operation. In the case of CP-823, CO conversion increased up to 10 cycles of DSS-like operation and maintained a high level even after 50 cycles. Although the initial activities of CP-823, HP-823, and SG-823 catalysts were lower than those of CP-1073, HP-1073, and SG-1073, respectively, after 10 cycles of DSS-like operation reversal of the relative activities was found. BET surface areas of HP-823 and SG-823 catalysts increased up to 10 cycles of DSS-like operation. In the case of CP-823, BET surface area increased up to 10 cycles of DSS-like operation and slightly decreased after 50 cycles. This suggests that the change in the structure of Cu/Al_2O_3 catalyst calcined at 823 K during the DSS-like operation affects the catalytic activity. CP-823 catalyst showed the highest activity among the Cu/Al_2O_3 catalysts tested. These results clearly demonstrate that the catalytic activity and sustainability against DSS-like operation are strongly affected by not only preparation method but also calcination temperature. The activities of CP-823, HP-823, and SG-823 catalysts were improved by DSS-like operation, suggesting that the homogeneity of the precursor has an important role in the preparation of highly sustainable catalyst.

3.3.Effect of DSS operation on the structure

Fig. 8 shows the XRD patterns of Cu/Al_2O_3 catalysts calcined at 823 and 1073 K after 10 cycles of DSS-like operation. CP-823, HP-823, and SG-823 reduced at 523 K showed the diffraction lines characteristic of Cu metal. The crystalline sizes of Cu metal in the catalysts were estimated to be 13 (CP-), 22 (HP-) and 23 (SG-) nm. After 10 cycles of DSS-like operation, the intensity and width of the diffraction lines of Cu metal were almost similar to those before the DSS-like operation, indicating that the sizes of Cu metal particles before DSS-like operation were almost similar to those after 10 cycles of DSS-like operation. The order of the crystalline sizes of Cu metal did not correspond with that of the activity. Many researchers have proposed that the activity of Cu-based catalyst depends on the Cu metal surface area [11, 12, 14, 16, 41, 42]. For example, the Cu metal surface areas of HP-Cu/ZnO, HP-Cu/ZnO/Al_2O_3, and HP-Cu/ZnO/MgO catalyst well correlated with the activities [16, 41]. Moreover, the catalytic activity correlates roughly with the Cu metal surface area after DSS-like operation (Fig. S3). Hence, an aggregation of a part of Cu metal may be one of the reasons for decreased activity for the WGS reaction resulting from DSS-like operation. In the case of CP-, HP-, and SG-823 (Figs. 8 (a), (b) and (c)), diffraction lines of boehmite (AlO(OH)) phase (JCPDS 21-1307) are

apparent. On the contrary, no diffraction line of boehmite was obtained in the XRD pattern of IMP-823 (Fig. 8 (d)). Moreover, Cu/Al_2O_3 catalysts calcined at 1073 K, which are remarkably deactivated by DSS-like operation as shown in Fig. 7, and Fig. 8(B) showed no diffraction lines of boehmite phase after 10 cycles of DSS-like operation in spite of the preparation method. Furthermore, in spite of calcination temperature, only the catalysts having diffraction lines of boehmite phase after 10 cycles of DSS-like operation indicated a high sustainability against DSS-like operations (Fig. S4). These results strongly indicate that boehmite has an important role in the sustainability against DSS operation. However, in the case of Cu/AlO(OH), CO conversion drastically decreased after 10 cycles of DSS-like operation (CO conversion decreased from 19 % to 4 %), suggesting that both close contact between Cu species and AlO(OH) is necessary to inhibit the deactivation during DSS operation. Fig. 9 shows the change in XRD patterns of CP- and IMP-Cu/Al_2O_3 calcined at 823 K against the cycles of DSS-like operation. In the case of IMP-823, no significant change in XRD pattern was observed. In contrast, in the case of CP-823, the diffraction lines of boehmite phase grew with the number of cycles of DSS-like operation.

The morphology of CP-823 and IMP-823 catalysts before and after DSS-like operation was investigated by TEM (Fig. 10). In the case of IMP-823 catalyst, no

significant change in the structure (rod-like crystals of γ-Al_2O_3) was observed after DSS-like operation (Fig. 10 (c) and (d)). In contrast, the TEM image of CP-823 catalyst after 50 cycles of DSS-like operation (Fig. 10 (b)) shows the formation of needle-like crystals, which is typical morphology for boehmite [42]. Furthermore, a number of small Cu species (ca. 15 nm) which was covered with boehmite looks like "bird's nest" together with a few large Cu metal particles (ca. 30 nm) was observed. This suggests that a few Cu metal particles were aggregated during DSS operation and the others which were covered with boehmite were inhibited from aggregation. IMP-Cu/AlO(OH) before and after 10 cycles of DSS-like operation showed needle-like crystals of boehmite whose size was much larger (Fig. S5) than that was formed on CP-823 after DSS-like operation (Fig. 10 (b)). The mean particle size of Cu metal was estimated to 36.0 nm from XRD patterns after 10 cycles of DSS-like operation and was much larger than that of CP-823.

According to above results, it can be concluded that inhibition of aggregation of Cu metal by "*in-situ*" formation of a small size of boehmite results in high sustainability against DSS operation.

3.4.TPR profiles of the catalysts before and after DSS operation

Fig. 11 shows TPR profiles of CP-823 and IMP-823 catalysts before and after a number of cycles of DSS-like operation. Freshly prepared IMP-823 catalyst shows a single H_2 consumption peak at 560 K with a small shoulder at 580 K (Fig. 11 B (a)), which is assignable to reduction of Cu^{2+} in bulk CuO to Cu^0 with a large distribution of particle size [14]. After reduction at 523 K, the H_2 consumption peak shifts to lower temperature (ca. 505 K) with a shoulder peak (ca. 470 K) (Fig. 11 B (b)). After 10 cycles of DSS-like operation, the amount of H_2 consumed is much smaller than that after the reduction. It seems that the H_2 consumption is caused by reduction of surface layer of or interfacial copper species oxidized during exposure to air at room temperature. When this sample was oxidized at 573 K, H_2 consumption peak around 525 K with a shoulder peak (ca. 470 K) is observed and the amount of H_2 consumed is recovered by ca. 85 % of the fresh catalyst (Fig. 11 B (c) thin line). This suggests that a most part of core of copper metal particles on IMP-823 was oxidized at 573 K. On the basis of these results, it appears that the copper metal particles on IMP-823 treated after 10 cycles of DSS-like operation is decorated with oxidized copper species. CP-823 catalyst shows two H_2 consumption peaks at 540 and 615 K (Fig. 11 A (a)). After reduction at 523 K, the H_2 consumption peak shifts to lower temperature (ca. 520 K) (Fig. 11 A (b)). After the 10 cycles of DSS-like operation,

the H_2 consumption peak also shifts to lower temperature (ca. 490 K) (Fig. 11 A (c)). The consumption of H_2 is almost similar to that of the catalyst reduced at 523 K. Agrell et al. reported that the peak of H_2-TPR shifted ca. 40 K toward lower temperature due to improvement the dispersion of copper on $Cu/ZnO/Al_2O_3$ [43]. Therefore, these results suggest that a part of copper species on CP-823 dispersed during the DSS-like operation up to 10 cycles. This may result in the increasing in the boundary between copper species and aluminum compounds. When this sample was oxidized at 573 K, CP-823 catalyst shows H_2 consumption peak at 515 K with two shoulder peaks (ca. 470 and 500 K) (Fig. 11 A (c) thin line). The ratio of the amount of H_2 consumed before and after oxidation at 573 K (2.7/4.3 = 0.63) is much larger than that of IMP-823 (0.5/4.6 = 0.11), indicating that the amount of copper species, which can be easily oxidized and reduced at low temperature, on CP-823 is much larger than that on IMP-823 after 10 cycles of DSS-like operation. These results also suggest that the boundary between copper species and aluminum compounds on CP-823 is much larger than that of IMP-823. Interestingly, the consumption of H_2 is constant up to 20 cycles of DSS-like operation (Fig. 11 A (d)), suggesting that aggregation of Cu metal particles does not occur during the DSS-like operation. This is cause by the inhibition of aggregation of Cu metal particles by boehmite

phase formed "*in-situ*" during the DSS operation.

3.5. *In-situ* time-resolved Cu K-edge XAFS

In-situ time-resolved Cu K-edge XANES spectra were measured to investigate the redox behavior of Cu species under reaction and DSS-like conditions. A factor analysis of the Cu K-edge XANES spectra revealed that three primary components were necessary to reconstruct the experimental XANES spectra. Cu^0, Cu_2O, and CuO were used as three probable reference compounds. Fig. 12 shows the change in Cu K-edge XANES spectra of CP-823 and IMP-823 during the DSS-like operation. Both CP-823 and IMP-823 show following behavior; Cu K-edge XANES spectra of both CP-823 and IMP-823 are similar to Cu metal (Fig. S6) under the WGS reaction condition before DSS-like operation. Then XANES spectra of CP-823 and IMP-823 are gradually changed, suggesting that a part of Cu metal was oxidized to Cu_2O and/or CuO (Fig. S6) under DSS-like operation. XANES spectra of CP-823 and IMP-823 after the 2nd WGS reaction after DSS-like operation are also similar to Cu metal, suggesting that most part of Cu species is present as Cu metal. To evaluate the fraction for each Cu species as a function of time, the spectra were analyzed by a liner combination method with Cu metal, Cu_2O, and CuO spectra as references. The

evolutions of the phase composition of CP-823 and IMP-823 catalysts are shown in Fig. 13. For CP-823, a most part of copper is present as Cu^0 under the WGS reaction condition. When a reaction mixture ($CO/CO_2/H_2O/H_2$ = 7.3/7.3/27.2/58.3) was changed to a mixture of H_2O/He (25.1/74.9), a part of Cu^0 was oxidized to Cu(I) and Cu(II). The fraction of Cu(I) increased with increasing the temperature and reached ca. 40 %. After a mixture of H_2O/He has been switched to the reaction mixture at 473 K, a rapid reduction of Cu(I) proceeded. In the case of IMP-823, a most part of copper is present as Cu^0 under the WGS reaction condition. When a reaction mixture was changed to a mixture of H_2O/He, a small part of Cu^0 was oxidized to Cu(I) and Cu(II) oxides. The fraction of Cu(I) slightly increased with increasing the temperature and reached ca. 12 %. After a mixture of H_2O/He has been switched to the reaction mixture at 473 K, a rapid reduction of Cu(I) proceeded. These results indicate that the amount of copper species ,which can be easily oxidized and reduced at low temperature, on CP-823 is much larger than that on IMP-823. This result corresponds with H_2-TPR results.

3.6. High sustainability of CP-823 against DSS operation

Surprisingly, the activity of CP-823 was greatly improved by DSS-like operation as

shown in Figs. 6 and 7. At the initial stage, the sustainability of this catalyst was superior to that of the commercial ternary $Cu/ZnO/Al_2O_3$ catalyst (MDC-7). To elucidate the sustainability of CP-823, a long-term life test of CP-823 catalyst was carried out. The change in CO conversion against the number of cycles of DSS operation was shown in Fig. 14. The activity was increasing up to 10 cycles, and no degradation was observed until 500 cycles of DSS operation. It is clearly shown that CP-823 is a highly active and sustainable catalyst against the DSS operations.

4. Conclusion

From above results, we conclude that CP-823 can act as a highly sustainable catalyst against the DSS-like operation in the WGS reaction. CP-823 showed high activity and sustainability even after 500 cycles of DSS operation. The high and stable activity of CP-823 is caused by the formation of highly dispersed and stable Cu metal. The important role of boehmite phase formed "*in-situ*" during the DSS operation in inhibition of aggregation of Cu metal particles was clearly demonstrated.

Acknowledgements

TS acknowledges the Grant-in-Aid for Scientific Research for Young Researchers (B) (No. 19760545) under the Ministry of Education, Culture, Sports Science and Technology (MEXT) of Japan. A part of this work is supported by the New Energy and Industrial Technology Development Organization (NEDO) in Japan. KT is supported by the Program for Improvement of Research Environment for Young Researchers from Special Coordination Funds for Promoting Science and Technology (SCF) commissioned by the Ministry of Education, Culture, Sports, Science and Technology (MEXT) of Japan.

References

[1] G. G. Scherer, Solid State Ionics 94 (1997) 249.

[2] S. Ahmed, M. Krumpelt, Int. J. Hydrogen Energy 26 (2001) 291.

[3] A. T. Ashcroft, Ak. K. Cheetham, J. S. Ford. M. L. H. Green, C. P. Grey, A. Murrell, P. D. F. Vernon, Nature 344 (1990) 259.

[4] J. R. Rostrup-Nielsen, Catal. Today 71 (2002) 243.

[5] K. Takehira, T. Shishido, Catal. Surv. Asia 11 (2007) 1.

[6] S. Liu, L. Xu, S. Xie, Q. Wang, G. Xiong, Appl. Catal. A 211 (2001) 145.

[7] N. M. Schmidt, P. Bröcheehoff, B. Höhlein, R. Menzer, U. Stimming, J. Power Sources 49 (1994) 299.

[8] F. Vidal, B. Busson, C. Six, O. Pluchery, A. Tadjeddine, Surf. Sci. 502-503 (2002) 485.

[11] M. J. L. Ginés, N. Amadeo, M. Laborde, C. R. Apesteguía. Appl. Catal. A 131 (1995) 283.

[12] K. Sekizawa, S.-I. Yano, K. Eguchi, H. Arai, Appl. Catal. A 169 (1998) 291.

[13] J. Wu, M. Saito, J. Catal. 195 (2000) 420.

[14] Y. Tanaka, T. Utaka, R.Kikuchi, K. Sasaki, K. Eguchi, Appl. Catal. A 242 (2003) 287.

[15] M. Rønning, F. Huber, H. Meland, H. Venvik, D. Chen, A. Holmen, Catal. Today, 100, (2005) 249.

[16] T. Shishido, M. Yamamoto, I. Atake, D. Li, Y. Tian, H. Morioka, M. Honda, T. Sano, K. Takehira, J. Mol. Catal. A 253 (2006) 270.

[17] Y. Tanaka, T. Takeguchi, R.Kikuchi, K. Eguchi, Appl. Catal. A 279 (2005) 59.

[18] T. Shishido, S. Nishimura, Y. Yoshinaga, K. Ebitani, K. Teramura, T. Tanaka, Catal. Commun., 10 (2009) 1057.

[19] Y. Li, Q. Fu, M. Flytzani-Stephanopoulos, Appl. Catal. B 27 (2000) 179.

[20] S. Hilaire, X. Wang, T. Luo, R.J. Gorte, J. Wagner, Appl. Catal A. 215 (2001) 271.

[21] T. Tabakova, F. Boccuzzi, M. Manzoli, D. Andreeva, Appl. Catal. A 252 (2003) 385.

[22] Q. Fu,W. Deng, H. Saltsburg, M. Flytzani-Stephanopoulos, Appl. Catal. B 56 (2005) 57.

[23] E.S. Bickford, S. Velu, C. Song, Catal. Today 99 (2005) 347.

[24] J.M. Zalc, V. Sokolovskii, D.G. Loffler, Appl. Catal. A 215 (2001) 271.

[25] P. Panagiotopoulou, D.I. Kondarides, J. Catal. 225 (2004) 327.

[26] T. Utaka, T. Takeguchi, R. Kikuchi, K. Eguchi, Appl. Catal. 246 (2003) 117.

[27] T. Utaka, T. Okanishi, T. Takeguchi, R. Kikuchi, K. Eguchi, Appl. Catal. A 245 (2003) 343.

[28] A. Venugopal, M.S. Scurrell, Appl. Catal. A 245 (2003) 137.

[29] Y. Tanaka, T. Utaka, T. Takeguchi, R.Kikuchi, K. Eguchi, Appl. Catal. A 238 (2003) 11.

[30] R.J. Candal, A.E. Regazzoni, M.A. Blesa, J. Mater. Chem. 2 (1992) 657.

[31] G.J. de A.A. Soler-Illia, R.J. Candal, A.E. Regazzoni, M.A. Blesa, Chem. Mater. 9 (1997) 184.

[32] H. Morioka, H. Tagaya, K. Karasu, J. Kadokawa, K. Chiba, J. Solid State Chem. 117 (1995) 337.

[33] T. Hayakawa, H. Harihara, A. G. Anderse, A. P. E. York, K. Suzuki, H. Yasuda, K. Takehira, Angew. Int. Chem. Int. Ed. 35 (1996) 192.

[34] K. Takrhia, T. Shishido, M. Kondo, J. Catal. 207 (2002) 307.

[35] J. W. Evans, M. S. Wainwright, A. J. Bridgewater. D. J. Young., Appl. Catal., 7 (1983) 75.

[36] A. Suzuki and M. Nomura, Proceedings of 9 th Japan XAFS society Annual meeting, 7O08.

[37] W. Ruettinger, O. Ilich, R. J. Farruato, J. Power Sorce 118 (2003) 61.

[38] H. Yahiro, K. Nakaya, T. Yamamoto, K. Saiki, H. Yamamura, Catal. Commun. 7 (2006) 228.

[39] F. Severino, J. L. Brito, J. Laine, J. L. G. Fierro, A.L. Agudo, J. Catal. 177 (1998) 82.

[40] M. F. Luo, P. Fang, M. He, Y. L. Xie, J. Mol. Catal. A 239 (2005) 243.

[41] T. Shishido, Y. Yamamoto, H. Morioka, K. Takaki, K. Takehira, Appl. Catal. A. 263 (2004) 249.

[42] H. Ivankovic, E. Tkalcec, R. Nass, H. Schmidt, J. Eur. Ceram. Soc. 23 (2003) 283.

[43] J. Agrell, H. Brigersson, M. Boutonnet, I. Melian-Cabrera, R. M. Navarro, J. L. G. Fierro, J. Catal. 219 (2003) 389.

Figure captions

Fig. 1. Diagram of DSS-like operation in the WGS reaction.

Fig. 2. Diagram of *in-situ* time-resolved XANES experiment.

Fig. 3. XRD patterns of Cu/Al_2O_3 catalysts calcined at various temperatures. (A) CP- and (B) IMP-, (a) before calcination, (b) calcined at 573 K, (c) 873 K, (d) 973 K, (e) 1023 K, (f) 1073 K, (g) 1173 K, (✳) hydrotalcite-like compound, (■) CuO, (○) $CuAl_2O_4$.

Fig. 4. TPR profiles of Cu/Al_2O_3 catalysts calcined at various temperatures. (A) CP- and (B) IMP-, (a) 823 K, (b) 873 K, (c) 973 K, (d) 1023 K, (e) 1073 K, (f) 1173 K. The numbers by peaks are the amount of H_2 consumed.

Fig. 5. Catalytic activity and Cu^0 surface area of Cu/Al_2O_3 catalysts as a function of calcination temperature. (A) CP- and (B) IMP-Cu/Al_2O_3. Reaction temperature 473 K, $CO/CO_2/H_2O/H_2$=7.3/7.3/27.2/58.3, GHSV=12.4 L h^{-1} g-cat^{-1}.

Fig. 6. Time course of CO conversion over Cu/Al_2O_3 catalysts, (A) before DSS-like operation and (B) after 10 cycles of DSS-like operation, (●) CP-823, (○) CP-1073, (▲) IMP-823, (△) IMP-1073, (✳) commercial $Cu/ZnO/Al_2O_3$ catalyst (MDC-7), Reaction temperature 473 K, $CO/CO_2/H_2O/H_2$=7.3/7.3/27.2/58.3, GHSV=12.4 L h^{-1} g-cat^{-1}.

Fig. 7. The change in catalytic activity in the water-gas shift reaction by the DSS-like operation over Cu/Al_2O_3, and commercial $Cu/ZnO/Al_2O_3$ (MDC-7) catalysts. Reaction temperature 473 K, $CO/CO_2/H_2O/H_2$=7.3/7.3/27.2/58.3, GHSV=12.4 L h^{-1} g-cat^{-1}.

Fig. 8. XRD patterns of Cu/Al_2O_3 catalysts after 10 cycles of DSS-like operation, (A) calcined at 823 K, (B) calcined at 1073 K, (a) CP-, (b) HP- (c) SG- and (d) IMP-Cu/Al_2O_3 catalysts. (□) Cu metal, (▼) AlO(OH), (○) $CuAl_2O_4$, (▽) γ-Al_2O_3.

Fig. 9. XRD patterns of (A) CP- and (B) IMP-Cu/Al_2O_3 catalysts, (a) calcined at 823 K, (b) reduced at 523 K, (c) after 1st DSS-like operation, (d) after 10 cycles of DSS, (e) after 20 cycles of DSS, and (f) after 50 cycles of DSS. (■) CuO, (□) Cu metal, (▼) AlO(OH), (▽) γ-Al_2O_3.

Fig. 10. TEM images of CP-823 and IMP-823 catalysts before and after DSS-like operation. (a) and (b), CP-823; (c) and (d), IMP-823.

Fig. 11. TPR profiles of CP-823 and IMP-823 catalysts before and after the DSS-like operation. (A) CP-823, (B) IMP-823. The numbers by peaks are the amount of H_2 consumed. (a) calcined at 823 K, (b) reduced at 523 K, (c) after 10 cycles of DSS, (d) after 20 cycles of DSS. The thin lines are TPR profiles of CP- and IMP-823, which were applied to 10 cycles of DSS-like operation, then were oxidized at 573 K.

Fig. 12. Cu K-edge XANES spectra of (A) CP-823 and (B) IMP-823 catalysts during the DSS-like operation. The diagram is shown in Fig. 2. The dashed line was under the WGS reaction condition, and the solid line was under the DSS-like operation.

Fig. 13. Evolution of Cu composition over the (A) CP-823 and (B) IMP-823 catalysts during DSS-like operation, (◇) Cu^0, (●) Cu^+, and (△) Cu^{2+}. The diagram is shown in Fig. 2.

Fig. 14. The change in catalytic activity of CP-823 catalyst against the DSS operations. Reaction condition; catalyst 10 cc, $CO/CO_2/H_2O/H_2$ (9.5/6.8/27.5/56.2), GHSV=700 h^{-1}, Reaction temperature 473 K.

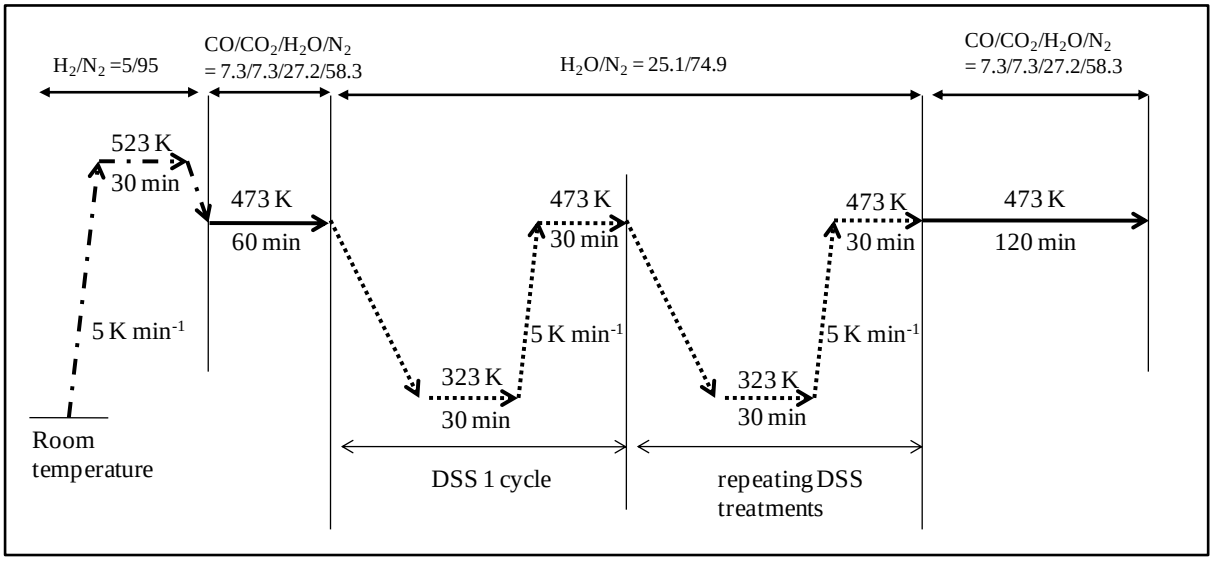

Fig. 1. Diagram of DSS-like operation in the WGS reaction.

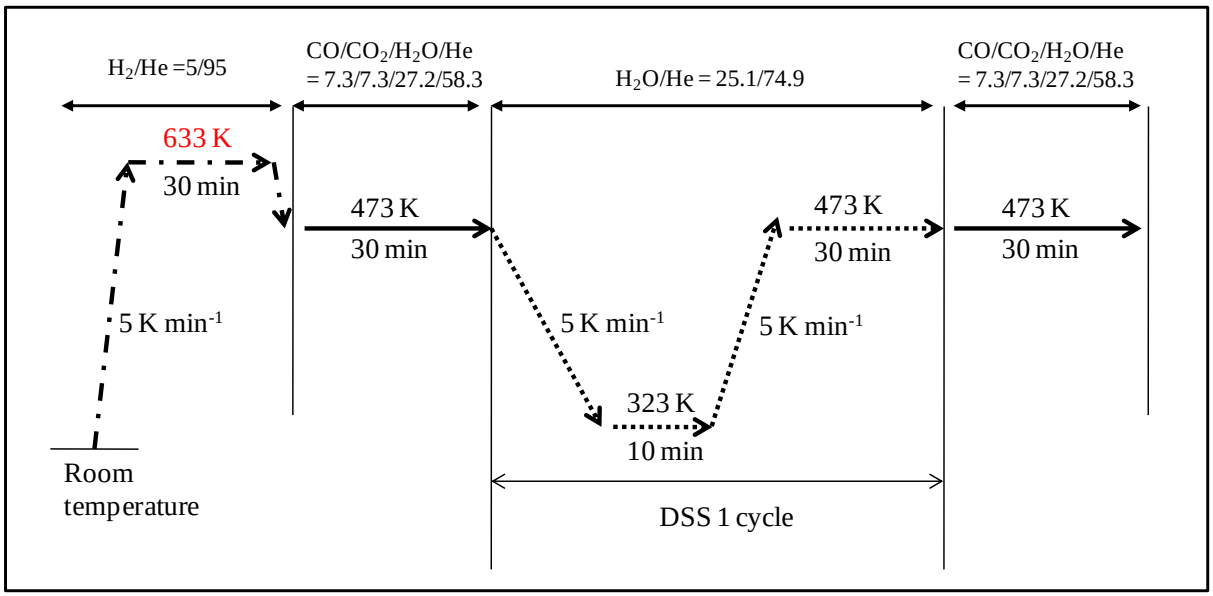

Fig. 2. Diagram of *in-situ* time-resolved XANES experiment.

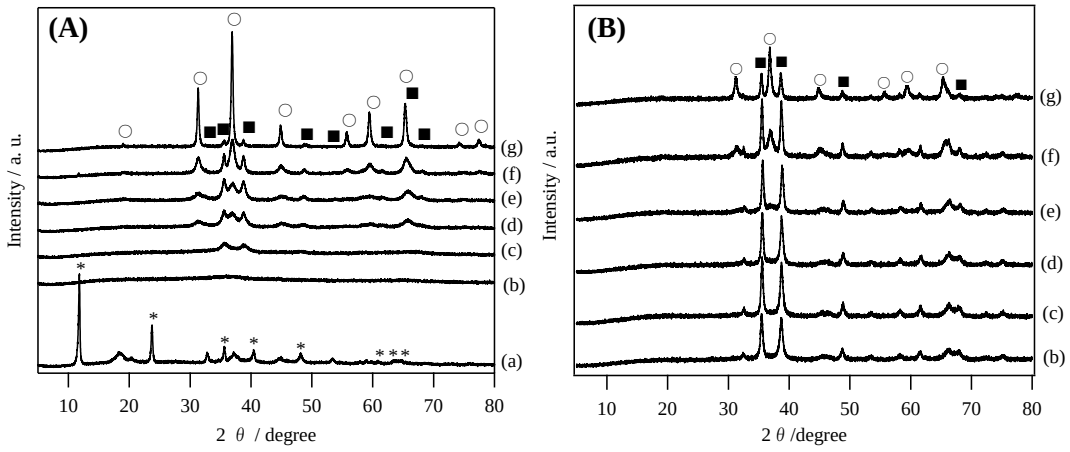

Fig. 3. XRD patterns of Cu/Al_2O_3 catalysts calcined at various temperatures. (A) CP- and (B) IMP-, (a) before calcination, (b) calcined at 573 K, (c) 873 K, (d) 973 K, (e) 1023 K, (f) 1073 K, (g) 1173 K, (✳) hydrotalcite-like compound, (■) CuO, (○) $CuAl_2O_4$.

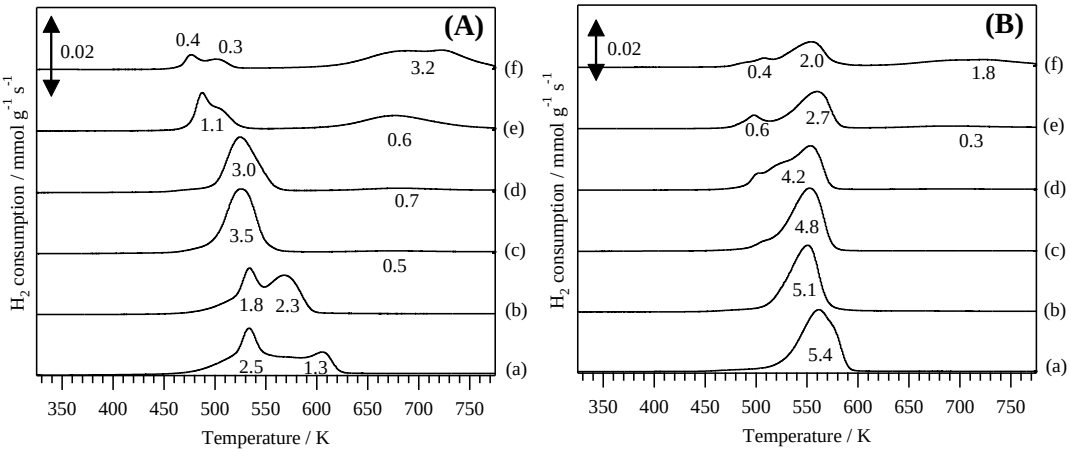

Fig. 4. TPR profiles of Cu/Al_2O_3 catalysts calcined at various temperatures. (A) CP- and (B) IMP-, (a) 823 K, (b) 873 K, (c) 973 K, (d) 1023 K, (e) 1073 K, (f) 1173 K. The numbers by peaks are the amount of H_2 consumed.

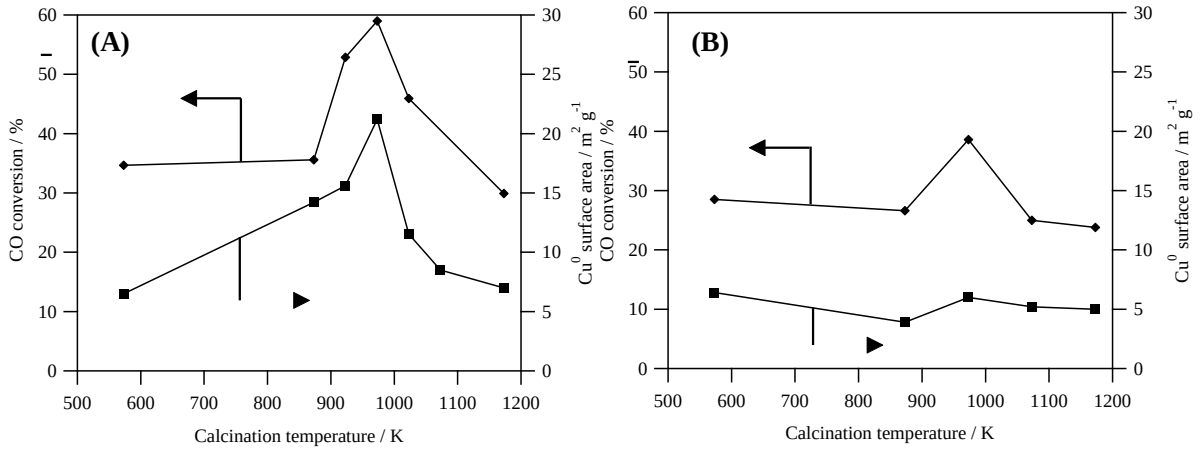

Fig. 5. Catalytic activity and Cu^0 surface area of Cu/Al_2O_3 catalysts as a function of calcination temperature. (A) CP- and (B) IMP-Cu/Al_2O_3. Reaction temperature 473 K, $CO/CO_2/H_2O/H_2$=7.3/7.3/27.2/58.3, GHSV=12.4 L h^{-1} g-cat^{-1}.

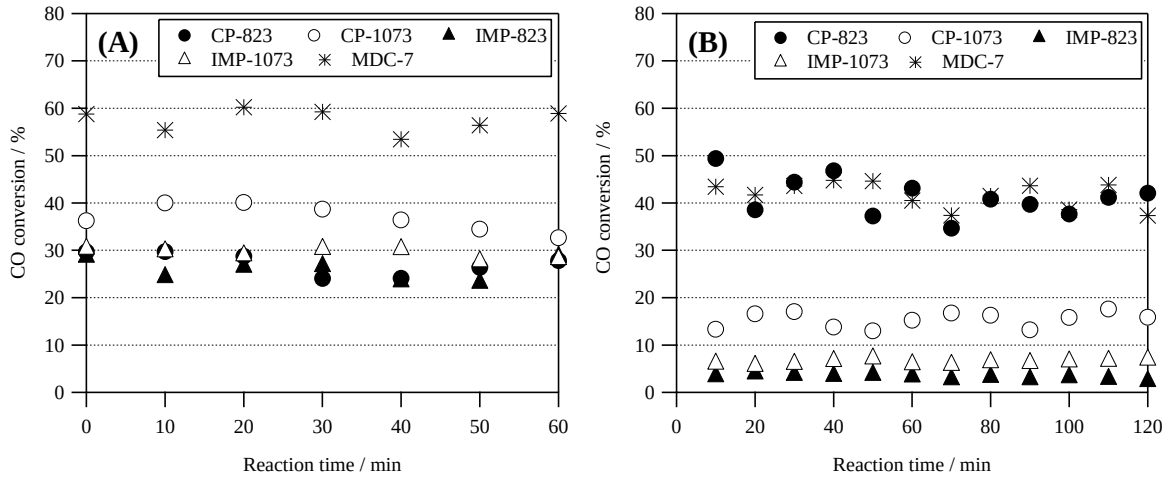

Fig. 6. Time course of CO conversion over Cu/Al_2O_3 catalysts, (A) before DSS-like operation and (B) after 10 cycles of DSS-like operation, (●) CP-823, (○) CP-1073, (▲) IMP-823, (△) IMP-1073, (✳) commercial $Cu/ZnO/Al_2O_3$ catalyst (MDC-7), Reaction temperature 473 K, $CO/CO_2/H_2O/H_2$=7.3/7.3/27.2/58.3, GHSV=12.4 L h^{-1} g-cat^{-1}.

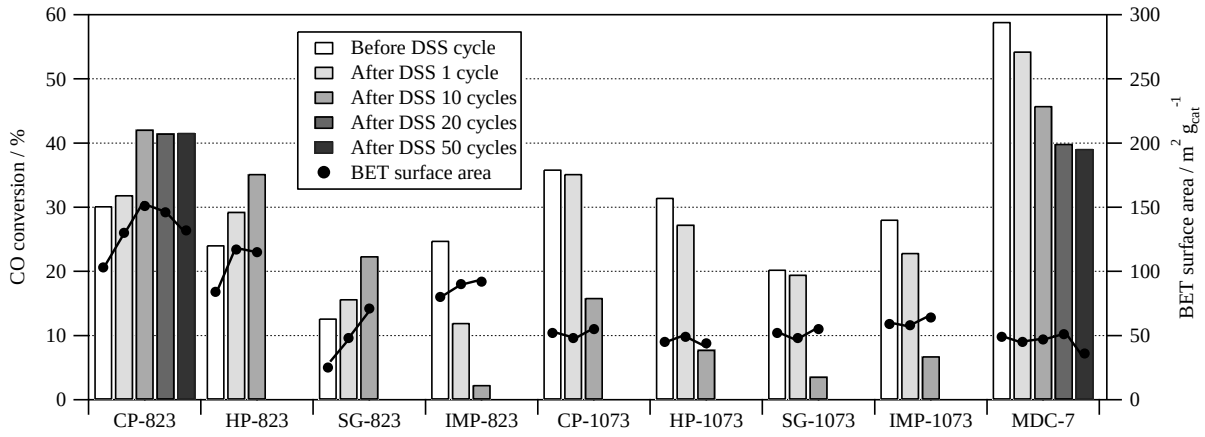

Fig. 7. The change in catalytic activity in the water-gas shift reaction by the DSS-like operation over Cu/Al_2O_3, and commercial $Cu/ZnO/Al_2O_3$ (MDC-7) catalysts. Reaction temperature 473 K, $CO/CO_2/H_2O/H_2$=7.3/7.3/27.2/58.3, GHSV=12.4 L h^{-1} g-cat^{-1}.

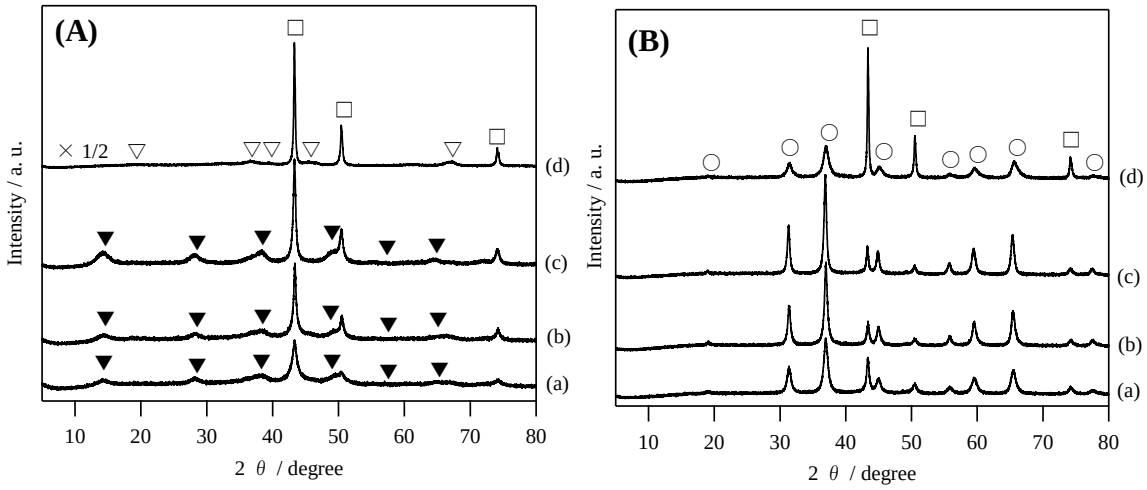

Fig. 8. XRD patterns of Cu/Al_2O_3 catalysts after 10 cycles of DSS-like operation, (A) calcined at 823 K, (B) calcined at 1073 K, (a) CP-, (b) HP- (c) SG- and (d) IMP-Cu/Al_2O_3 catalysts. (□) Cu metal, (▼) AlO(OH), (○) $CuAl_2O_4$, (▽) γ-Al_2O_3.

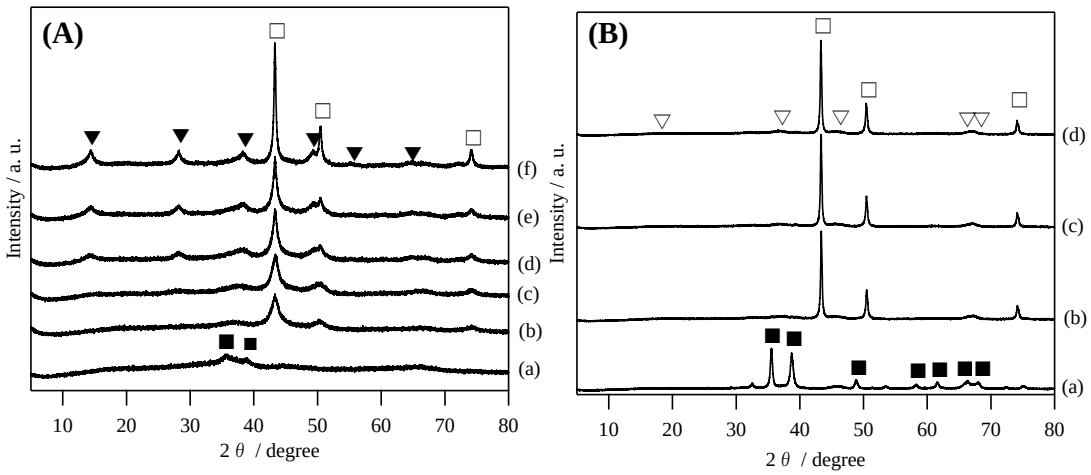

Fig. 9. XRD patterns of (A) CP- and (B) IMP-Cu/Al_2O_3 catalysts, (a) calcined at 823 K, (b) reduced at 523 K, (c) after 1st DSS-like operation, (d) after 10 cycles of DSS, (e) after 20 cycles of DSS, and (f) after 50 cycles of DSS. (■) CuO, (□) Cu metal, (▼) AlO(OH), (▽) γ-Al_2O_3.

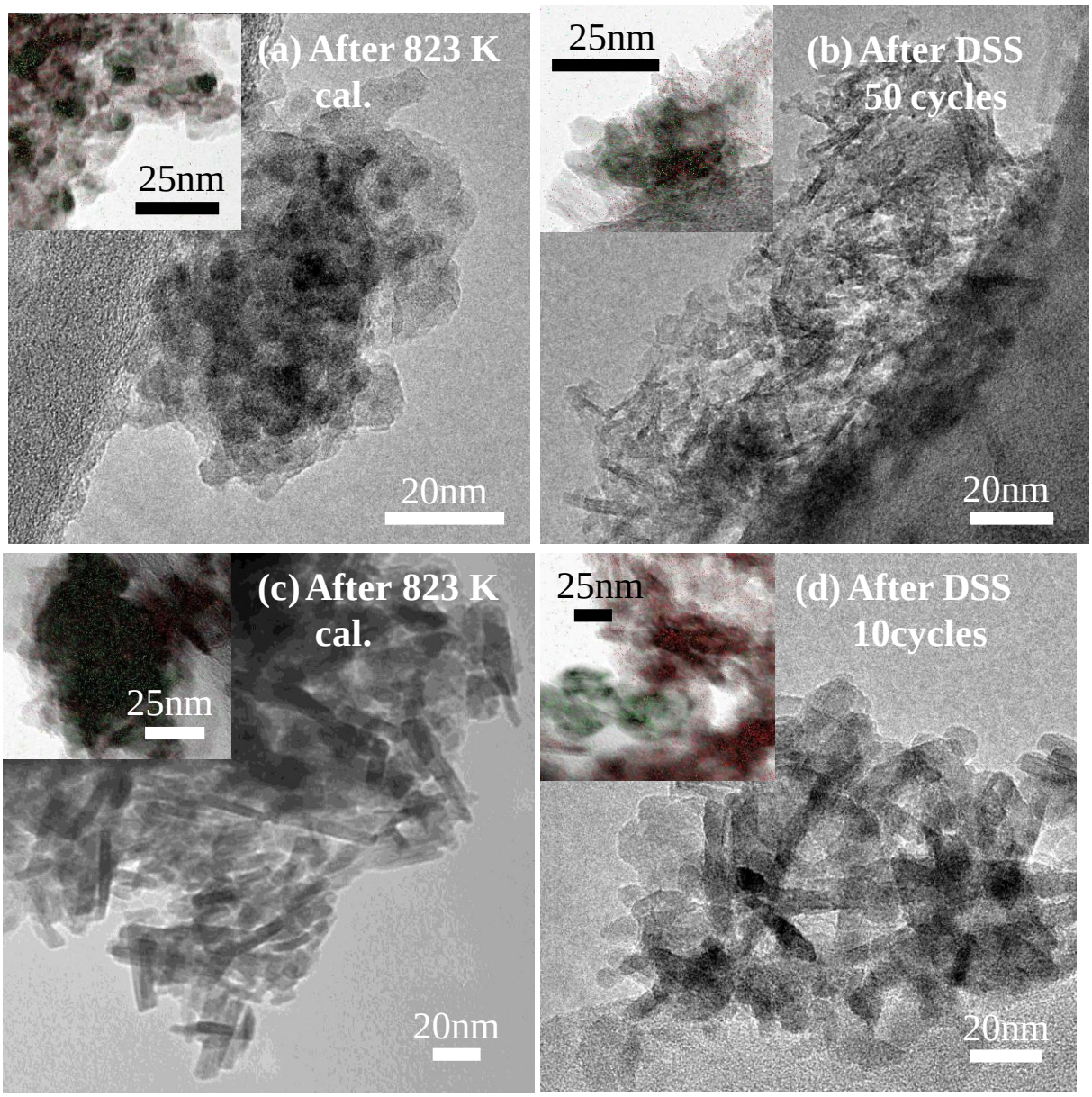

Fig. 10. TEM images of CP-823 and IMP-823 catalysts before and after DSS-like operation. (a) and (b), CP-823; (c) and (d), IMP-823.

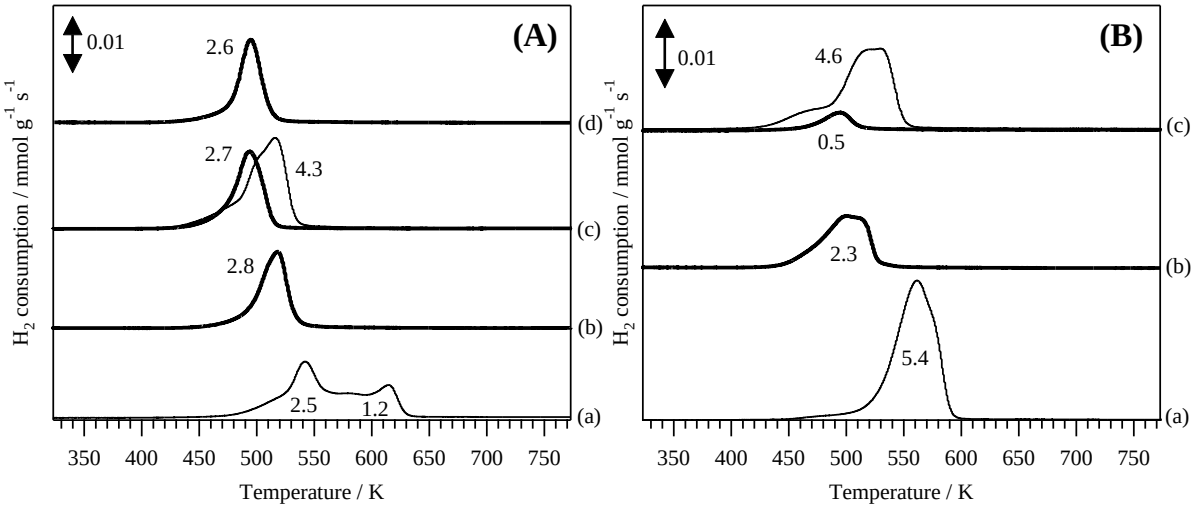

Fig. 11. TPR profiles of CP-823 and IMP-823 catalysts before and after the DSS-like operation. (A) CP-823, (B) IMP-823. The numbers by peaks are the amount of H_2 consumed. (a) calcined at 823 K, (b) reduced at 523 K, (c) after 10 cycles of DSS, (d) after 20 cycles of DSS, The thin lines are TPR profiles of CP- and IMP-823, which were applied to 10 cycles of DSS-like operation, then were oxidized at 573 K.

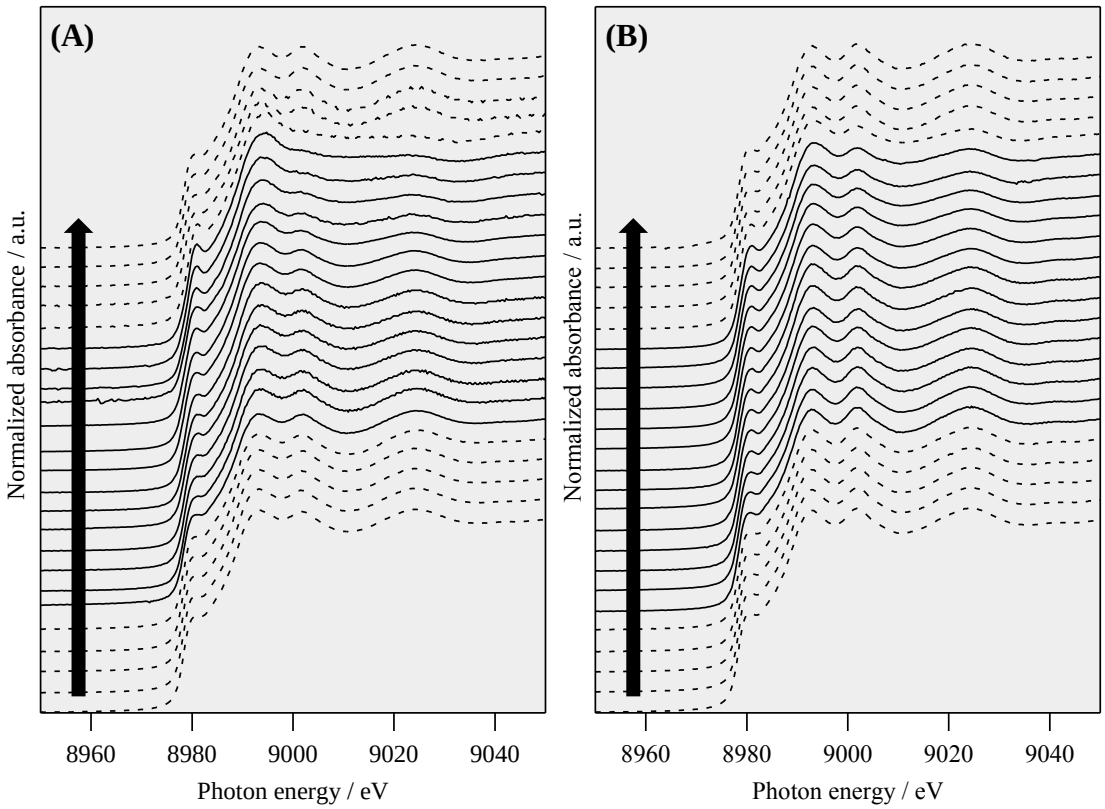

Fig. 12. Cu K-edge XANES spectra of (A) CP-823 and (B) IMP-823 catalysts during the DSS-like operation. The diagram is shown in Fig. 2. The dashed line was under tha WGS reaction condition, and the solid line was under the DSS-like operation.

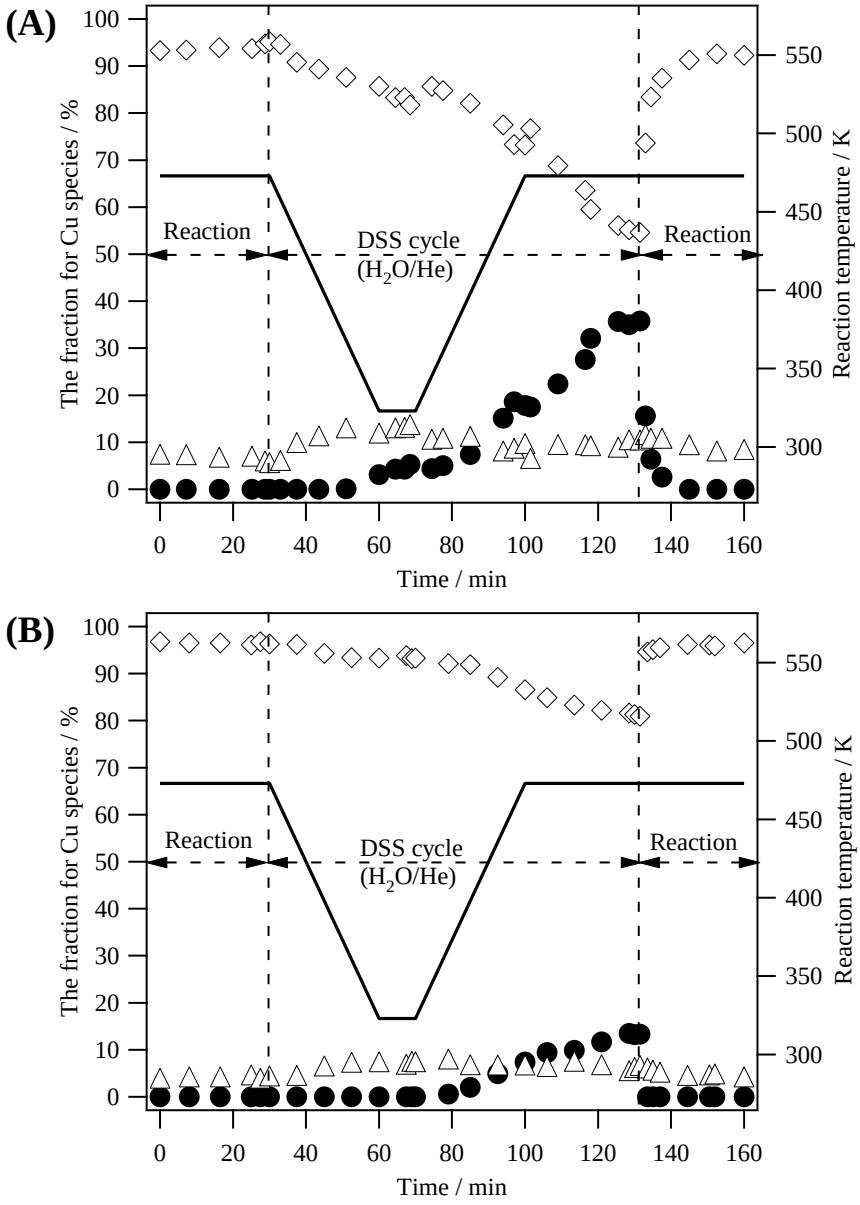

Fig. 13. Evolution of Cu composition over the (A) CP-823 and (B) IMP-823 catalysts during DSS-like operation, (◇) Cu^0, (●) Cu^+, and (△) Cu^{2+}. The diagram is shown in Fig. 2.

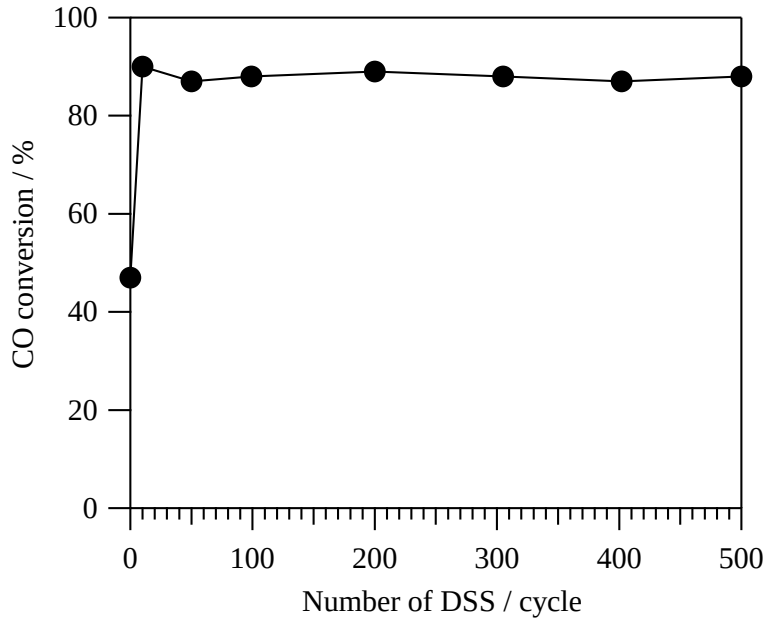

Fig. 14. The change in catalytic activity of CP-823 catalyst against the DSS operations. Reaction condition; catalyst 10 cc, $CO/CO_2/H_2O/H_2$ (9.5/6.8/27.5/56.2), GHSV=700 h^{-1}, Reaction temperature 473 K.

Supporting Information for

Novel catalytic behavior of Cu/Al_2O_3 catalyst against daily start-up and shut-down (DSS)-like operation in the water gas shift reaction

Shun Nishimura,[b] Tetsuya Shishido,*[a] Kohki Ebitani,[b] Kentaro Teramura,[c]

and Tsunehiro Tanaka[a]

[a] *Department of Molecular Engineering, Graduate School of Engineering, Kyoto University, Katsura, Kyoto 615-8510, Japan.*
[b] *School of Materials Science, Japan Advanced Institute of Science and Technology, Nomi, Ishikawa 923-1292, Japan.*
[c] *Kyoto University Pioneering Research Unit for Next Generation, Kyoto University, Katsura, Kyoto 615-8510, Japan.*

Corresponding author

Dr. Tetsuya Shishido
Department of Molecular Engineering, Graduate School of Engineering, Kyoto University,
Katsura, Kyoto 615-8510, Japan.
Tel: +81 75 383 2559
Fax: +81 75 383 2561
E-mail: shishido@moleng.kyoto-u.ac.jp

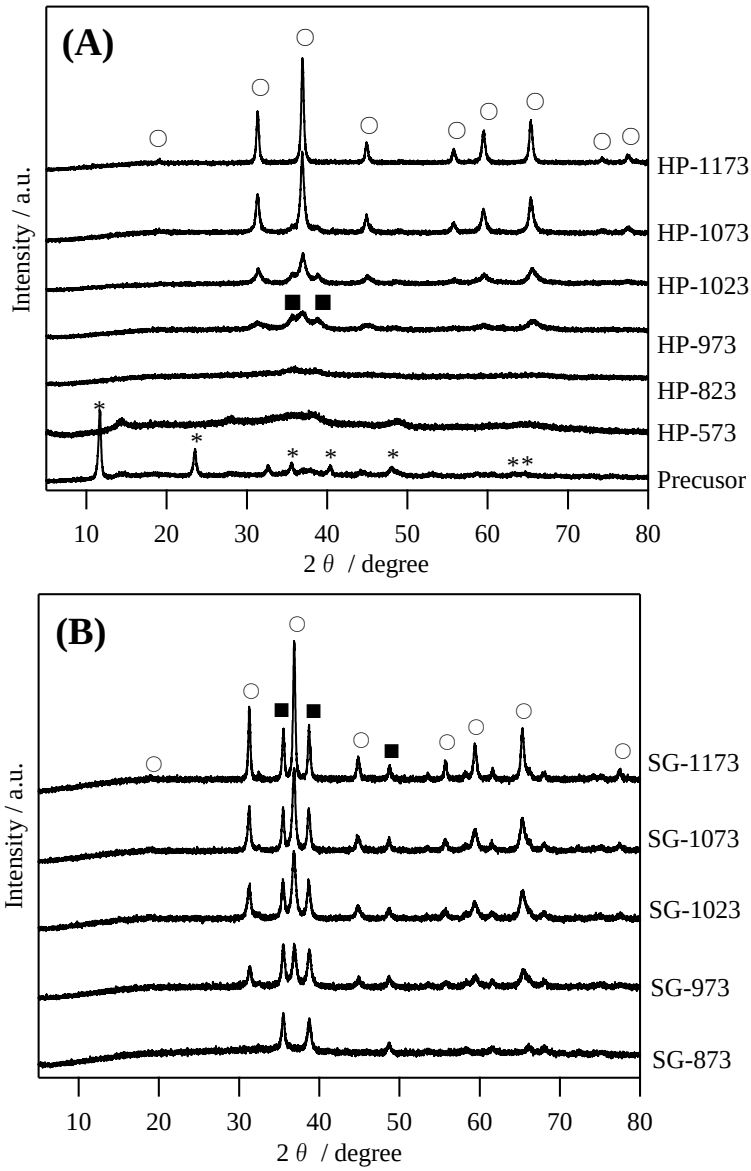

Fig. S1. XRD patterns of Cu/Al_2O_3 catalysts calcined at various temperatures. (A) HP- and (B) SG-Cu/Al_2O_3, (✳) hydrotalcite–like compund, (■) CuO, (○) $CuAl_2O_4$.

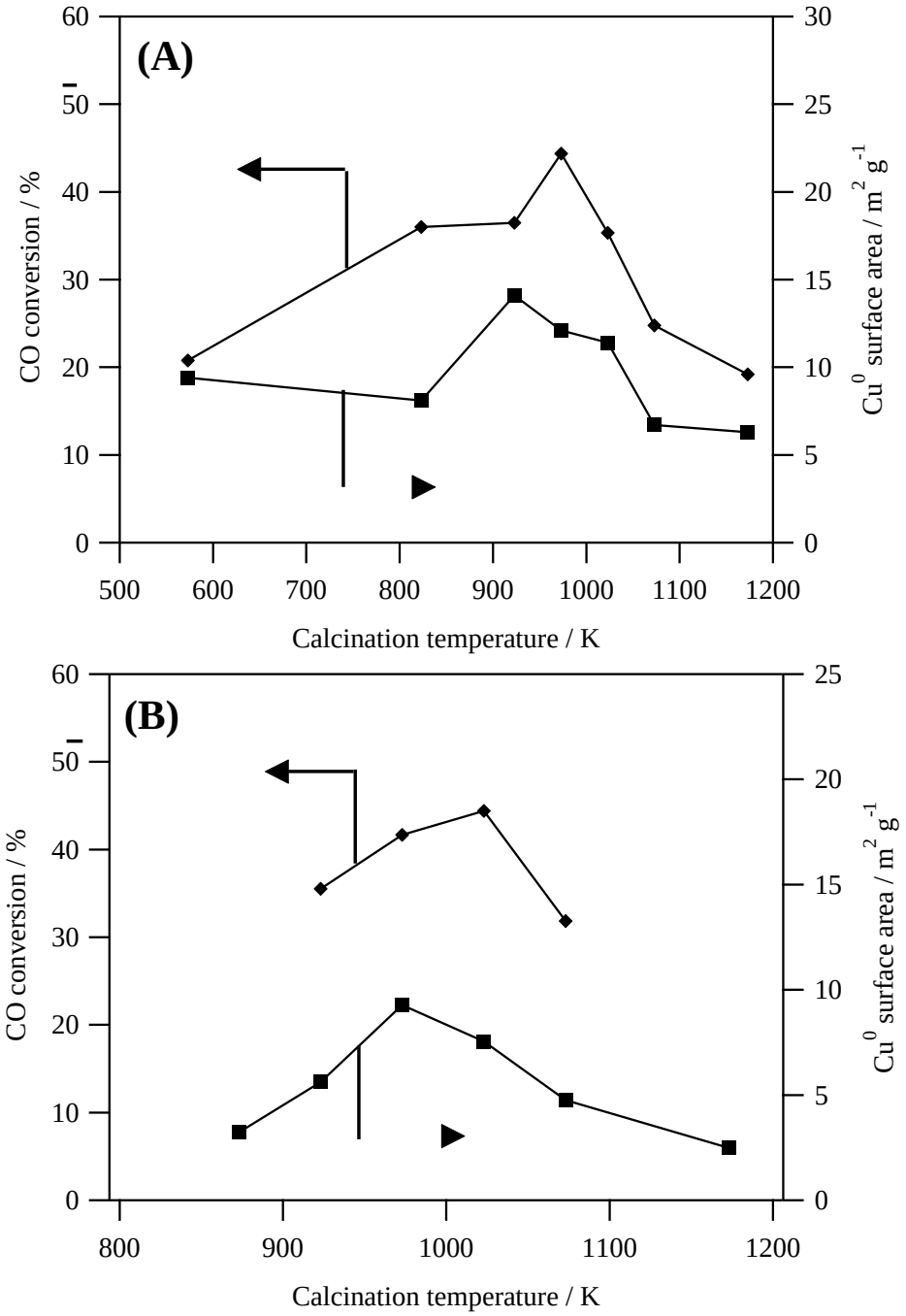

Fig. S2. Catalytic activity and Cu^0 surface area of Cu/Al_2O_3 catalysts as a function of calcination temperature. (A) HP- and (B) SG-Cu/Al_2O_3. Reaction temperature 473 K, $CO/CO_2/H_2O/H_2$=7.3/7.3/27.2/58.3, GHSV=12.4 L h^{-1} g-cat^{-1}.

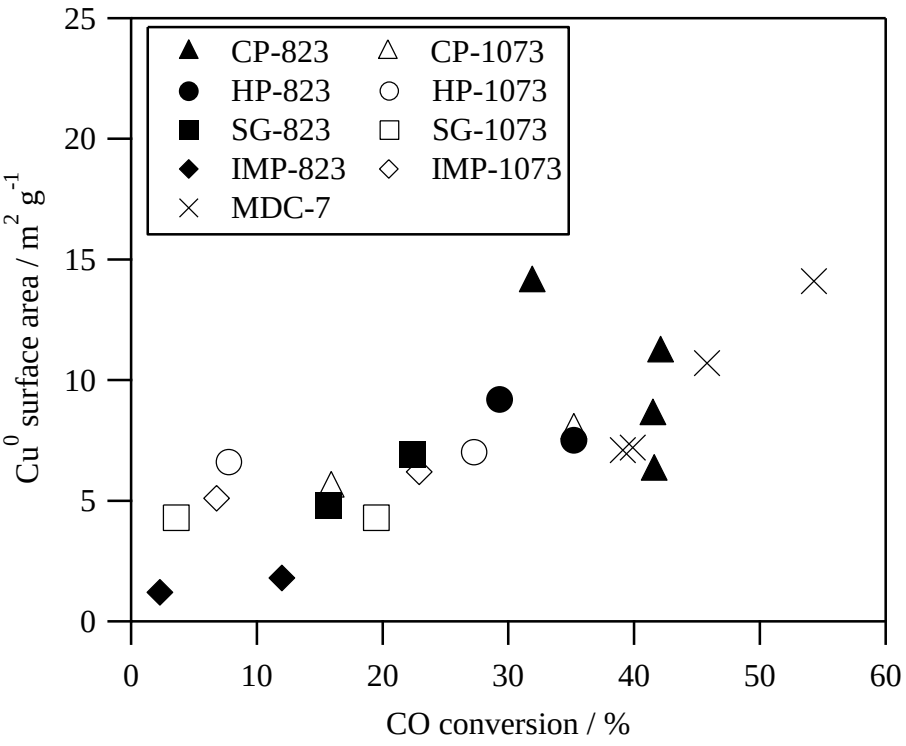

Fig. S3. The relationship between the catalytic activities and Cu metal surface area of the samples after DSS-like operations.

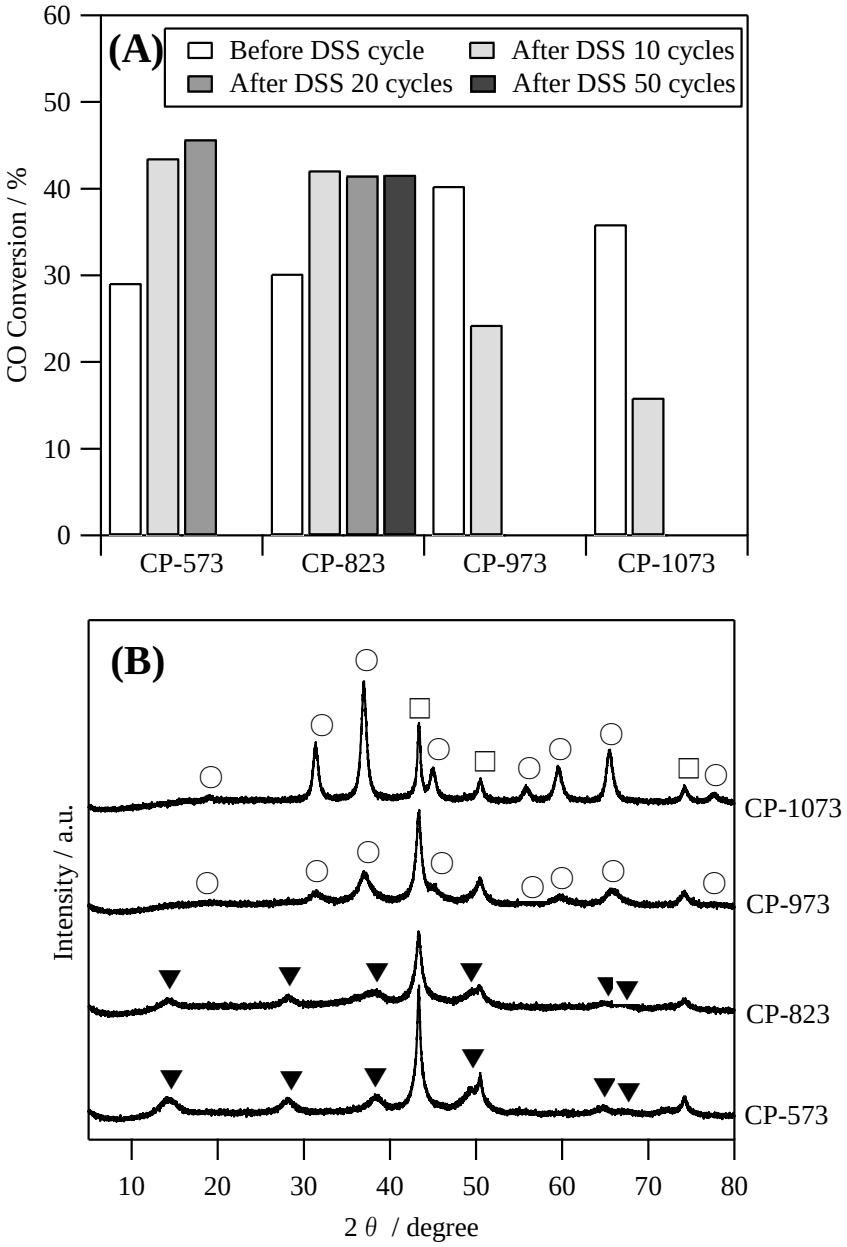

Fig. S4.

(A) The change in catalytic activity in the water-gas shift reaction by the DSS-like operation over CP-Cu/Al_2O_3 calcined at various temperatures. Reaction temperature 473 K, CO/CO_2/H_2O/H_2=7.3/7.3/27.2/58.3, GHSV=12.4 L h^{-1} g-cat^{-1}. (B) XRD patterns of CP-Cu/Al_2O_3 calcined at various temperature after 10 cycles of DSS operation, (□) Cu metal, (▼) AlO(OH), (◯) $CuAl_2O_4$.

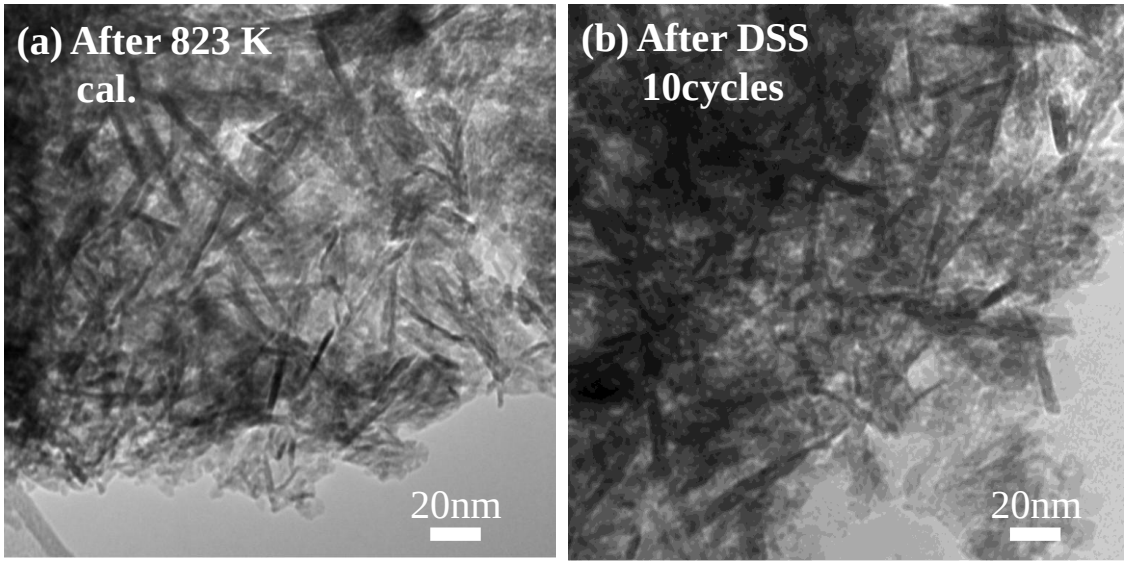

Fig. S5. TEM images of IMP-Cu/AlO(OH) catalysts before and after 10 cycles of DSS-like operation.

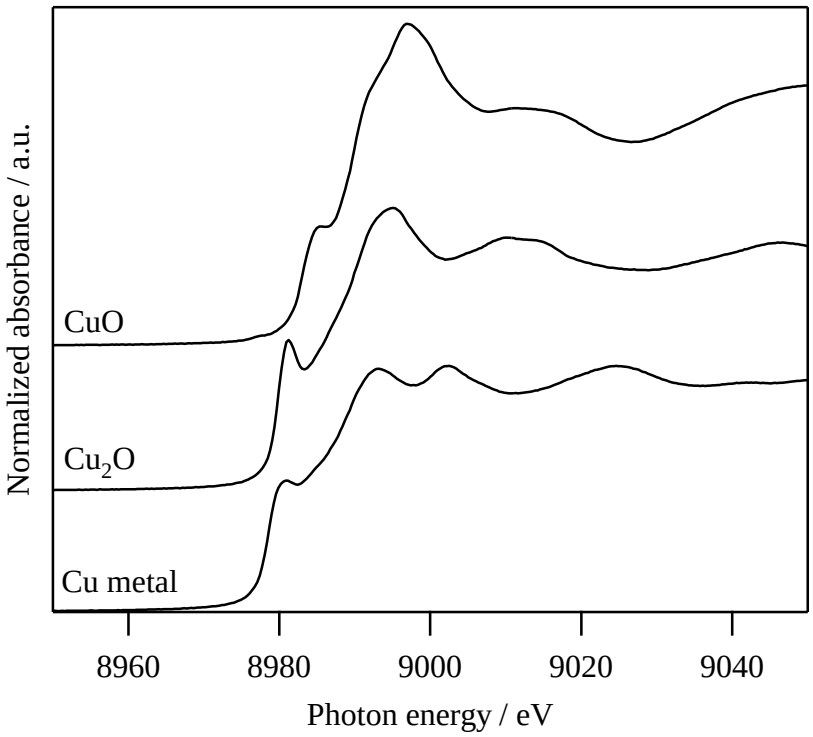

Fig. S6. Cu K-edge XANES spectra of Cu metal, Cu_2O, and CuO used as references.